Bull. Mater. Sci., Vol. 39, No. 6, October 2016, pp. 1435–1440. © Indian Academy of Sciences.
DOI 10.1007/s12034-016-1299-3

Effect of 'Al' concentration on spin-dependent resonant tunnelling in InAs/Ga$_{1-y}$Al$_y$As symmetrical double-barrier heterostructures

L BRUNO CHANDRASEKAR[1,*], K GNANASEKAR[1], M KARUNAKARAN[2] and R CHANDRAMOHAN[3]
[1]Department of Physics, The American College, Madurai 625002, India
[2]Department of Physics, Alagappa Arts College, Karaikudi 630003, India
[3]Department of Physics, Sree Sevugan-Annamalai College, Devakottai 630303, India

MS received 29 April 2015; accepted 11 April 2016

Abstract. **The effect of 'Al' concentration on spin-dependent tunnelling in strained non-magnetic symmetric double-barrier semiconductor has been theoretically investigated. The separation between spin-up and spin-down components, barrier transparency, polarization efficiency and tunnelling lifetime were calculated using the transfer matrix approach. The separation between spin-up and spin-down resonances and tunnelling lifetime were reported for the first time in the case of InAs/Ga$_{1-y}$Al$_y$As heterostructures for various 'Al' concentrations and for various barrier widths. Cent percentage polarization can be obtained in this strained non-magnetic double-barrier semiconductor even without any external field.**

Keywords. **Spin–orbit interaction; barrier transparency; polarization efficiency; tunnelling lifetime.**

1. Introduction

The spin–orbit interaction, which couples the electron spin and the electron orbital motion, plays a significant role in spintronics devices [1]. The spin–orbit interaction is caused due to bulk inversion and structure inversion asymmetry. Both the Dresselhaus effect due to bulk inversion asymmetry and the Rashba effect due to structure inversion asymmetry are key to generate spin current in nanostructures. In the symmetrical structure, the total spin–orbit interaction is only due to Dresselhaus spin–orbit interaction [2–4]. Many efforts have been made to generate spin current in nanostructures. After the notable work by Tsu and Esaki [5], resonant double-barrier tunnel structures have gained more attention globally for both science and technological applications.

In this article, we have considered III–V rectangular non-magnetic symmetry double-barrier structures. The rectangular double-barrier heterostructures are extensively studied for two reasons, such as its mathematical simplicity and experimental data consistency [6]. The in-plane components can play a well-defined role in the transmission due to the existence of a discontinuity in the electronic band parameters at the tunnel structure interfaces and due to the dependence of an electronic effective mass on space position [7–10].

The rectangular non-magnetic symmetrical double-barrier heterostructures are considered, such as InAs–Ga$_{1-y}$Al$_y$As–InAs–Ga$_{1-y}$Al$_y$As–InAs, to calculate the separation between spin-up and spin-down resonances, barrier transparency, polarization efficiency and tunnelling lifetime of electrons, due to Dresselhaus spin–orbit interaction, using the transfer matrix approach. Lack of data on 'Al' concentration-dependent energy separation between spin resonances and tunnelling lifetime of electrons for the above-mentioned system has led to carry out this work.

The proposed model to calculate the barrier transparency and polarization efficiency with bulk inversion asymmetry is given in section 2, using the transfer matrix approach and the spin-dependent boundary conditions. The results of the numerical calculations and the discussions are given in section 3 followed by conclusion.

2. Model

We consider a double-potential barrier system as shown in figure 1. V is the potential of the barrier and a and c are the barrier widths in the regions 2 and 4, respectively. m_{j} is the effective mass of an electron in the jth region.

Since we consider the symmetry double barrier, $a = c$ and $m_2 = m_4$. The electron motion in each layer of the structure is described by the Hamiltonian,

$$H = -\frac{\hbar^2}{2m}\frac{\partial^2}{\partial z^2} + \frac{\hbar^2 k_{\parallel}^2}{2m} + V(z) + H_{\mathrm{D}}, \tag{1}$$

where m is the effective mass of an electron in the conduction band, $k_{||}$ the wave vector in the plane of interfaces, $V(z)$ the heterostructure potential and H_{D} the spin-dependent Dresselhaus term. Assuming that the kinetic energy of incident

---

[*] Author for correspondence (brunochandrasekar@gmail.com)

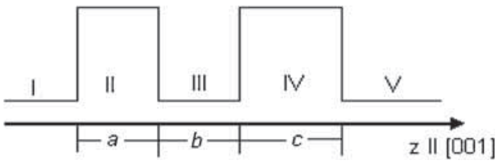

Figure 1. Electron transmission through [001] grown double-barrier structure.

electron is less than the barrier height, the Dresselhaus term is described as follows [6],

$$\begin{aligned} H_{\mathrm{D}} &= \gamma\left[\sigma_x k_x - \sigma_y k_y\right]\frac{\partial^2}{\partial z^2} \\ &= \gamma\left[\begin{pmatrix} 0 & 1 \\ 1 & 0 \end{pmatrix} k_x - \begin{pmatrix} 0 & -i \\ i & 0 \end{pmatrix} k_y\right]\frac{\partial^2}{\partial z^2}, \end{aligned} \tag{2}$$

where γ is the material constant and σ's are Pauli's spin matrices.

The unitary matrix is formed using the spinor $\chi = \frac{1}{\sqrt{2}}\begin{pmatrix} 1 \\ \pm e^{-i\theta} \end{pmatrix}$ such as [10],

$$U = \frac{1}{\sqrt{2}}\begin{pmatrix} 1 & 1 \\ -e^{-i\theta} & e^{-i\theta} \end{pmatrix}. \tag{3}$$

The Dresselhaus term is diagonalized by the unitary transformation,

$$H_{\mathrm{D}}^{(d)} = U^{+} H_{\mathrm{D}} U \tag{4}$$

$$= \begin{pmatrix} -\gamma k_{\parallel}\frac{\partial^2}{\partial z^2} & 0 \\ 0 & \gamma k_{\parallel}\frac{\partial^2}{\partial z^2} \end{pmatrix}. \tag{5}$$

For the fixed in-plane wave vector, the wavefunctions of the electrons are of the form

$$\Psi_{\pm}(\vec{r}) = \chi_{\pm} u_{\pm}(z)\exp(i\vec{k}_{\parallel}\vec{\rho}), \tag{6}$$

where $\vec{\rho}$ is an in-plane coordinate of the barrier. Here '+' and '−' correspond to spin-up and spin-down states of an electron, respectively. The electron propagations through the double barrier are described in the regions I, II, III, IV and V as below:

$$\begin{aligned} &u_{\pm}^{(I)}(z) = A_{\pm}^{(I)}\exp[ik_z(z-z_1)] + B_{\pm}^{(I)}\exp[-ik_z(z-z_1)], \\ &u_{\pm}^{(II)}(z) = A_{\pm}^{(II)}\exp[q_{\pm}(z-z_2)] + B_{\pm}^{(II)}\exp[-q_{\pm}(z-z_2)], \\ &u_{\pm}^{(III)}(z) = A_{\pm}^{(III)}\exp[ik_z(z-z_3)] + B_{\pm}^{(III)}\exp[-ik_z(z-z_3)], \\ &u_{\pm}^{(IV)}(z) = A_{\pm}^{(IV)}\exp[q_{\pm}(z-z_4)] + B_{\pm}^{(IV)}\exp[-q_{\pm}(z-z_4)], \\ &u_{\pm}^{(V)}(z) = A_{\pm}^{(V)}\exp[ik_z(z-z_5)]. \end{aligned}$$

With the diagonalized spin–orbit coupling term, the electron behaviour in barrier region is described by [10]

$$\frac{d^2 u_{\pm}(z)}{dz^2} - q_{\pm} u_{\pm}(z) = 0, \tag{7}$$

where $q_{\pm}$ is the wave vector through the barrier region. The wave vector for Dresselhaus spin–orbit interaction is given by [10]

$$q_{\pm} = \frac{q_0}{\sqrt{1 \pm \gamma^2 m_2 k_{\parallel}/\hbar^2}}, \tag{8}$$

where q_0 is the reciprocal length of decay of the wavefunction in the barrier region when the spin–orbit interactions are neglected and it is given by [10,11]

$$q_0 = \sqrt{\frac{2m_2 V}{\hbar^2} - k_z^2\frac{m_2}{m_1} - k_{\parallel}^2\left(\frac{m_2}{m_1} - 1\right)}. \tag{9}$$

According to the boundary conditions, the interface matrix S_i for the first and third interfaces ($j = 1, 3$) is given by

$$S_i = \frac{1}{2}\begin{pmatrix} 1 & \left(\frac{m_j}{ik_z}\right) \\ 1 & \left(\frac{-m_j}{ik_z}\right) \end{pmatrix} \times \begin{pmatrix} \exp(q_{\pm}(z_j - z_{j+1})) & \exp(-q_{\pm}(z_j - z_{j+1})) \\ \left(\frac{q_{\pm}}{m_{j+1}}\right)\exp(q_{\pm}(z_j - z_{j+1})) & \left(\frac{-q_{\pm}}{m_{j+1}}\right)\exp(-q_{\pm}(z_j - z_{j+1})) \end{pmatrix}. \tag{10}$$

Similarly, across the second and fourth interfaces ($j = 2, 4$) the interface matrix is given below.

$$S_i = \frac{1}{2}\begin{pmatrix} 1 & \left(\frac{m_j}{q_{\pm}}\right) \\ 1 & \left(\frac{-m_j}{q_{\pm}}\right) \end{pmatrix} \times \begin{pmatrix} \exp(ik_z(z_j - z_{j+1})) & \exp(-ik_z(z_j - z_{j+1})) \\ \left(\frac{ik_z}{m_{j+1}}\right)\exp(ik_z(z_j - z_{j+1})) & \left(\frac{-ik_z}{m_{j+1}}\right)\exp(-ik_z(z_j - z_{j+1})) \end{pmatrix}. \tag{11}$$

The continuity conditions across the boundaries would give the following.

$$\begin{pmatrix} A_{\pm}^{(V)} \\ 0 \end{pmatrix} = S_4 . S_3 . S_2 . S_1 \begin{pmatrix} A_{\pm}^{(I)} \\ B_{\pm}^{(I)} \end{pmatrix}, \tag{12}$$

where S_1, S_2, S_3 and S_4 are transfer matrices across different interfaces whose elements are calculated by applying the continuity conditions across the respective interfaces. The barrier transparency is given by

$$T_{\pm} = \left|A_{\pm}^{(V)}\right|^2. \tag{13}$$

The polarization efficiency P can be determined using the below expression

$$P = \frac{|T_{+}| - |T_{-}|}{|T_{+}| + |T_{-}|}. \tag{14}$$

We used this equation to calculate the spin-dependent polarization efficiency of the non-magnetic double-barrier semiconductor.

Table 1. Parameters used in calculations.

‘Al’ concentration (%)	$m_1 = m_3 = m_5$ (m_0)	$m_2 = m_4$ (m_0)	V (meV)
20	0.023	0.084	677.36
30	0.023	0.092	765.53
40	0.023	0.100	858.57

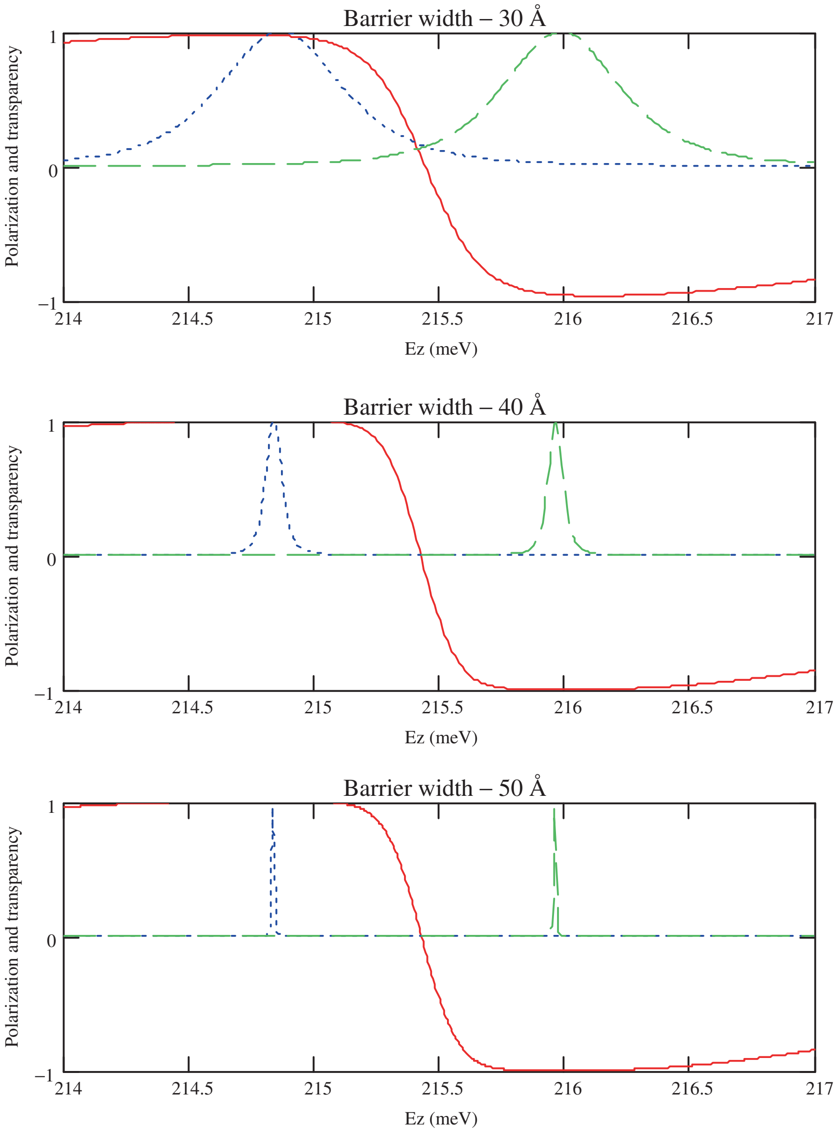

Figure 2. Polarization and transparency as a function of longitudinal energy in InAs–$Ga_{0.8}Al_{0.2}As$–InAs–$Ga_{0.8}Al_{0.2}As$–InAs heterostructure.

3. Results and discussion

The barrier transparency and the spin-dependent polarization efficiency of the strained symmetry non-magnetic double-barrier semiconductor with fixed $k_{||} = 2 \times 10^8$ m^{-1} is calculated as a function of longitudinal energy of the incident electron. For all our calculations the well width between the barriers is taken as 50 Å and γ is 24 eV Å^3 [12]. The other parameters used in our calculations are given in table 1 [10,13–15].

Figures 2–4 show the barrier transparency and polarization efficiency in InAs/$Ga_{1-y}Al_yAs$ heterostructures for various ‘Al’ concentrations. The figures clearly indicate that one can obtain the maximum or cent percentage polarization without any external field in the case of strained heterostructures even when the barrier width is small, such as 30 Å. This

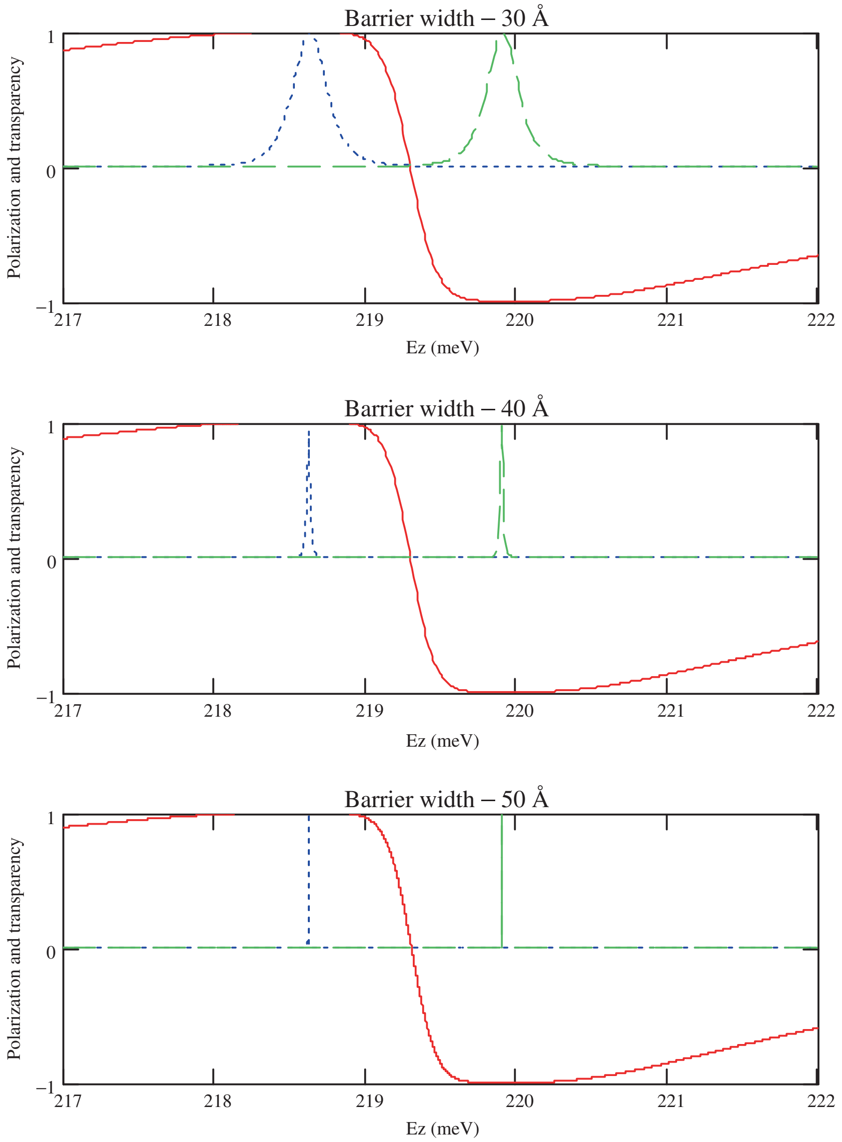

Figure 3. Polarization and transparency as a function of longitudinal energy in InAs–$Ga_{0.7}Al_{0.3}As$–InAs–$Ga_{0.7}Al_{0.3}As$–InAs heterostructure.

may be due to the band discontinuity at the tunnel structure interfaces and the very high potential of the barrier in the case of strained heterostructures. By increasing the 'Al' concentration, the resonance polarization shifts to the higher longitudinal energy of the incident electron.

Moreover, we investigated the energy separation between spin resonances as a function of 'Al' concentration in InAs/$Ga_{1-y}Al_yAs$ heterostructures. It is interesting to note that the separation between the spin-up and spin-down components increases linearly as the barrier height increases and the same decreases as the barrier width increases. The calculated values are graphically shown in figure 5. Though the separation between spin components decreases as the barrier width increases, the deviation is noted to be very small.

Gnanasekar and Navaneethakrishnan [10] also observed cent percent polarization without any external field in the case of strained heterostructures. Their calculations show that in the case of InAs/GaSb double-barrier heterostructures the polarization efficiency is 60–70% with Dresselhaus spin–orbit interaction, 75–85% with in-plane Rashba spin–orbit interaction and almost cent percent with both interactions. However in this present study, our calculations indicate that Dresselhaus spin–orbit interaction alone can cause polarization efficiency of 100% in InAs/$Ga_{1-y}Al_yAs$ heterostructures.

In order to understand tunnelling properties more clearly in the case of InAs/$Ga_{1-y}Al_yAs$ heterostructures for various 'Al' concentrations, the tunnelling lifetime has been calculated. The tunnelling lifetime, which is also known as lifetime of quasibound level, can be calculated from the equation [13], $\tau = \hbar/\Delta E$, where ΔE is the full-width at half-maximum of resonant peaks according to different spin

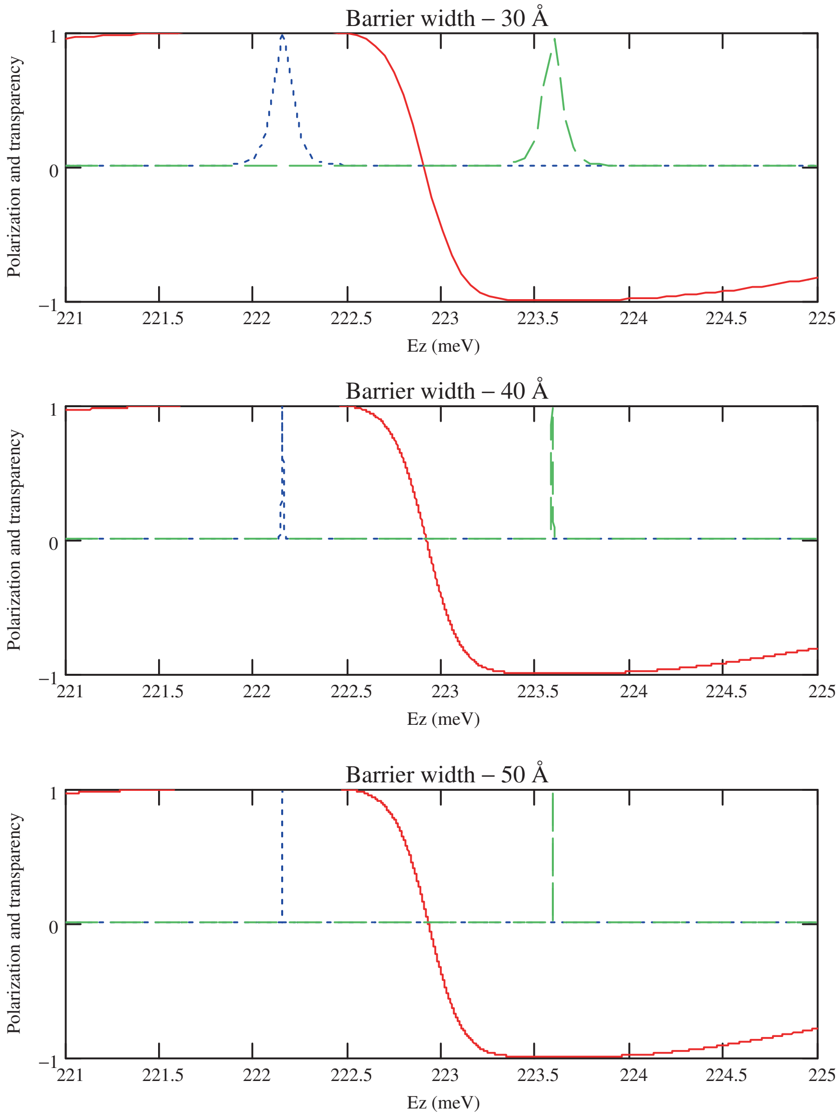

Figure 4. Polarization and transparency as a function of longitudinal energy in InAs–$Ga_{0.6}Al_{0.4}As$–InAs–$Ga_{0.6}Al_{0.4}As$–InAs heterostructure.

states. As 'Al' concentration increases, the tunnelling lifetime of electrons increases nonlinearly. This is true irrespective of the barrier width. The calculated values are graphically shown in figure 6. There are no other results available to compare with our results.

For $k_{||} = 2 \times 10^8$ m^{-1}, the tunnelling lifetime of spin-up and spin-down electrons are equal. The in-plane wave vector other than 2×10^8 m^{-1}, tunnelling lifetime of spin-up and spin-down electrons are different [13]. To summarize our results, as 'Al' concentration increases in InAs/$Ga_{1-y}Al_yAs$ heterostructures, (i) the separation between spin resonances increases linearly and (ii) the tunnelling lifetime of spin-polarized electrons increases nonlinearly. Moreover, one can reach 100% polarization efficiency in the case of considered strained symmetric semiconductor heterostructures, as Dresselhaus spin–orbit coupling is relatively strong in GaAs and $Ga_{1-y}Al_yAs$. These ideas and results could be employed in spin-dependent optoelectronic devices and it is believed that

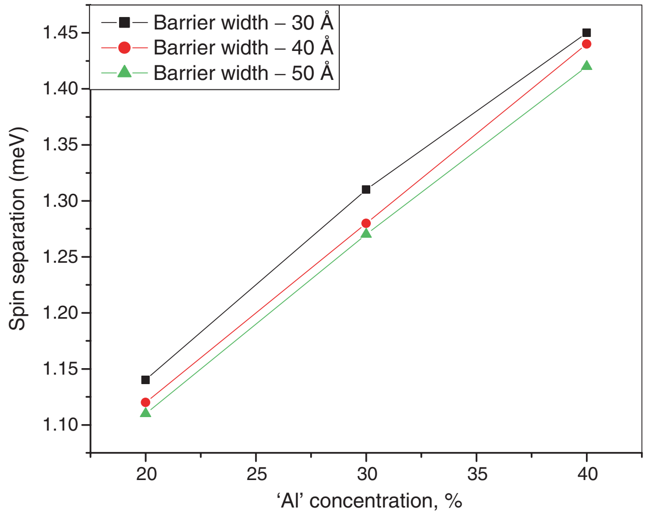

Figure 5. Spin separation *vs.* 'Al' concentration.

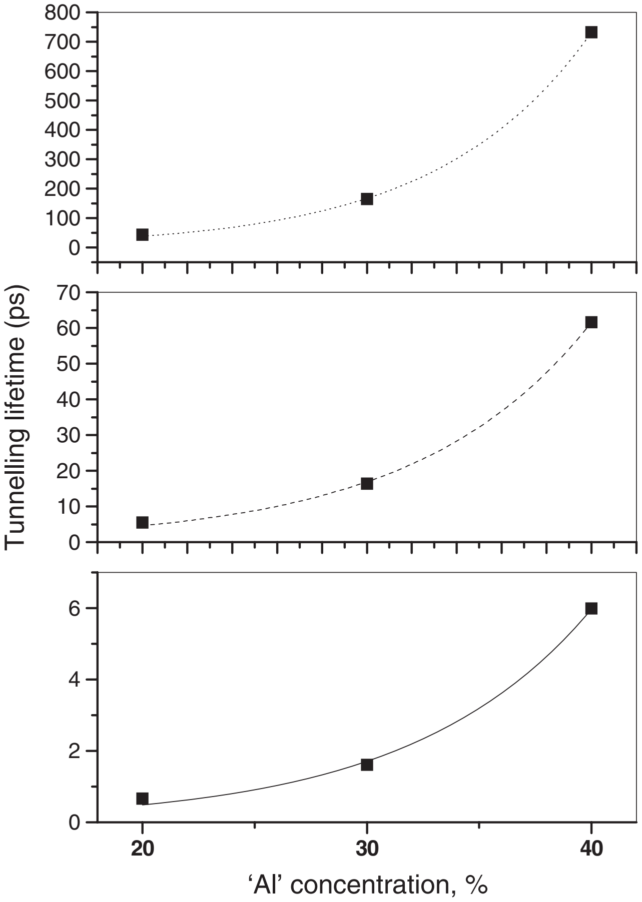

Figure 6. Tunnelling lifetime *vs.* 'Al' concentration for the barrier width of 30 Å (solid line), 40 Å (dash line) and 50 Å (dot line).

this work will trigger the researcher towards further studies in the field of spintronics.

4. Conclusion

The barrier transparency, energy separation between the spin resonances, polarization efficiency and tunnelling lifetime are calculated for symmetry strained heterostructures. The energy separation between spin-up and spin-down resonances and tunnelling lifetime are reported for the first time in InAs/$Ga_{1-y}Al_yAs$ heterostructures. The linear increased spin separation and nonlinearly increased tunnelling lifetime are observed as the 'Al' concentration increases. It is estimated and concluded that 100% polarization is possible to be achieved even without any external field in the case of this strained system. The result suggests that these systems are suitable for the fabrication of spin devices.

References

[1] Yang W, Chang K and Zhang S C 2008 *Phys. Rev. Lett.* **100** 056602

[2] de Andrada eSilva E A, La Rocca G C and Bassani F 1994 *Phys. Rev. B* **50** 8523

[3] Dresselhaus G 1955 *Phys. Rev.* **100** 580

[4] Rashba E I 1960 *Sov. Phys. Solid State* **2** 1109

[5] Tsu R and Esaki L 1973 *Appl. Phys. Lett.* **22** 562

[6] Wang H, Xu H and Zhang Y 2006 *Phys. Lett. A* **355** 481

[7] Paranjape V V 1995 *Phys. Rev. B* **52** 10740

[8] Wang X H, Gu B Y and Yang G Z 1997 *Phys. Rev. B* **55** 9340

[9] Voskoboynikov A, Liu S S and Lee C P 1999 *Phys. Rev. B* **59** 12514

[10] Gnanasekar K and Navaneethakrishnan K 2005 *Physica E* **28** 328

[11] Perel V I, Tarasenko S A, Yassievich I N, Ganichev S D, Bel'kov V V and Prettl W 2003 *Phys. Rev. B* **67** 201304

[12] Perel V I, Tarasenko S A, Yassievich I N, Ganichev S D, Bel'kov V V and Prettl W 2003 *Phys. Rev. B* **67** 201304(R)

[13] Gong J, Liang X X and Ban S L 2007 *J. Appl. Phys.* **102** 073718

[14] Gerardin Jayam Sr and Navaneethakrishnan K 2003 *Solid State Comm.* **126** 681

[15] Gnanasekar K and Navaneethakrishnan K 2005 *Phys. Lett. A* **341** 495